

Translocation of polymers into crowded media with dynamic attractive nanoparticlesWei-Ping Cao,^{1,2} Qing-Bao Ren,² and Meng-Bo Luo^{1,3,*}¹*Department of Physics, Zhejiang University, Hangzhou 310027, China*²*Department of Physics, Lishui University, Lishui 323000, China*³*Collaborative Innovation Center of Advanced Microstructures, Nanjing University, Nanjing 210093, China*

(Received 5 February 2015; revised manuscript received 2 June 2015; published 29 July 2015)

The translocation of polymers through a small pore into crowded media with dynamic attractive nanoparticles is simulated. Results show that the nanoparticles at the *trans* side can affect the translocation by influencing the free-energy landscape and the diffusion of polymers. Thus the translocation time τ is dependent on the polymer-nanoparticle attraction strength ε and the mobility of nanoparticles V . We observe a power-law relation of τ with V , but the exponent is dependent on ε and nanoparticle concentration. In addition, we find that the effect of attractive dynamic nanoparticles on the dynamics of polymers is dependent on the time scale. At a short time scale, subnormal diffusion is observed at strong attraction and the diffusion is slowed down by the dynamic nanoparticles. However, the diffusion of polymers is normal at a long time scale and the diffusion constant increases with the increase in V .

DOI: [10.1103/PhysRevE.92.012603](https://doi.org/10.1103/PhysRevE.92.012603)

PACS number(s): 83.80.Sg, 87.15.A–, 87.15.H–

I. INTRODUCTION

The translocation of polymer chains through small pores is a ubiquitous process in chemical and biological systems. Important examples include DNA and RNA worming through nuclear pores [1], DNA molecules transferring from virus to host cell [2], and protein transporting through membrane channels [3]. Polymer translocation has a lot of technological applications, such as rapid DNA sequencing and gene therapy [4,5], controlled drug delivery [6], size exclusion chromatography [7], etc. Since the process of polymer translocation is important in science and technology, it has been studied extensively in experiments [4,5,8–10], theories [11–16], and computer simulations [17–33].

The process of polymer translocation is dependent on many factors, such as pore structure [8,9,20], polymer-pore interaction [8,15,20,26,29,33], solvent properties [27], polymer concentration [22,28], and so on. However, one can qualitatively understand the behavior of polymer translocation from two important ingredients: the free-energy landscape [14,17] and the external driving force [34,35]. For the polymer threading through a nanopore from the *cis* side to the *trans* side, the loss of available conformations leads to a free-energy barrier, which prevents the translocation and dramatically affects the translocation dynamics. In contrast, the electric field [11,12], chemical potential difference [4], or binding proteins at the *trans* side [36,37] can impose an extra driving force on the polymer translocation by tilting the free-energy landscape. The translocation of polymers is also influenced by the environment. Crowding such as macromolecules and other inclusions, which are called nanoparticles (NPs) here, in cellular cytoplasm may result in a huge volume percentage [38]. Neutral or repulsive NPs in the system can reduce the entropy of polymers due to the excluded volume (EV) effect. Theoretical study showed that the translocation dynamics was influenced by static or dynamic repulsive NPs, and the

translocation time was dependent on the concentrations of NPs at the *cis* side ϕ_c as well as at the *trans* side ϕ_t [39]. Novel scaling behaviors of the translocation time τ on the polymer length N , such as a weak dependence $\tau \sim N$ at $\phi_c \gg \phi_t$ and a strong dependence $\tau \sim \exp(N)$ for dynamic NPs and $\tau \sim \exp(N^{0.6})$ for static ones at $\phi_t \gg \phi_c$, were observed by using the Fokker-Planck equation [39].

In addition to the EV effect of NPs, polymer-NP attraction would also change the free-energy landscape of polymer translocation, and thus it affects the translocation property of polymers [40–43]. Both the dynamic Monte Carlo (MC) simulation and the Langevin dynamics (LD) simulation showed that the polymer-NP attraction could obviously change the translocation time of polymers. The attractive NPs at the *trans* side could draw the polymer through the pore by lowering the energy, and thus decrease the translocation time [40]. However, the diffusion rate of polymers was slowed down at strong polymer-NP attraction because the polymers were adsorbed on NPs, thus the translocation time was significantly increased at strong polymer-NP attraction. This resulted in a special attraction strength at which the translocation was fastest. There was another attractive strength at which the attraction compensated for the EV of NPs, thus the translocation time was roughly independent of the NP concentration.

Recently, an LD simulation was carried out for the translocation of a two-dimensional flexible polymer into crowded media with dynamic NPs at the *trans* side [41]. Results showed that the translocation probability can be improved by increasing the binding energy between polymers and NPs. The translocation time rapidly decreases and then almost saturates with increasing binding energy for short chains, and it has a minimum for longer chains. The simulation for the translocation of stiff polymers also confirmed that the mean translocation time showed a minimum as a function of the binding energy and particle concentration [42]. The asymmetric size of the crowding agents at both sides during polymer translocation were investigated using both theoretical analysis and LD simulations in two-dimensional systems [43]. It was found that polymers preferred to translocate into the side with bigger NPs. The probability of polymer translocation

*Author to whom all correspondence should be addressed: luomengbo@zju.edu.cn

initially increased rapidly and then saturated with the increase in the area fraction of NPs, but it had a maximum with the increase in the sizes of NPs at the *trans* side. In contrast, the translocation time decreased with the increase in the area fraction of NPs, but it had a minimum with the increase in the size of NPs.

In this paper, we focus our simulation study on the effects of dynamic NPs at the *trans* side on the translocation of self-avoiding polymers by using a three-dimensional (3D) dynamic MC simulation. The MC method was shown to be an efficient way to simulate the translocation of polymers [17,23,30,40,44]. Mobile but self-avoiding NPs are placed only at the *trans* side. The interaction between polymers and NPs and the NP mobility are taken into account. Since there is only one interaction parameter in our system, it is easy for us to analyze the results and uncover the main factors affecting the physical picture of the translocation. Results show that there exists an optimal attraction between polymers and NPs at which the translocation time is minimum. On the other hand, the dynamics of NPs will affect the translocation of polymers by influencing the contact between polymers and NPs. An interesting observation is that τ increases with V in a power-law relation at small V but decreases in a power-law relation at large V . To understand the effect of NPs on translocation, the conformation and diffusion properties of a polymer chain in the crowding media with dynamic NPs are also simulated. We find that both the conformation and diffusion properties are deeply influenced by polymer-NP interaction and NP mobility. Another interesting result is that the effect of attractive dynamic NPs on the dynamics of polymers is dependent on the time scale. At a short time scale, subnormal diffusion is observed at strong attractions and the diffusion is slowed down by the dynamic NPs. However, diffusion of polymers is normal at a long time scale, and the diffusion constant increases with an increase in NP mobility.

II. MODEL AND SIMULATION METHOD

Our model system for polymer translocation is embedded in the 3D simple cubic (sc) lattice. In the present model, a self-avoiding walk (SAW) polymer chain of length N is comprised of N self-avoiding identical segments, and each segment occupies one lattice site. The bond length can vary from 1 to $\sqrt{3}$ on the sc lattice. The dynamic NP is represented by a unit cube occupying eight lattice sites. NPs are only placed at the *trans* side. Figure 1 presents a sketch showing a polymer chain translocating through a pore to enter the *trans* side filled with dynamic NPs. The model system and simulation method are briefly described in the following.

An infinitely large flat membrane at $x = 0$, perpendicular to the x direction, divides the simulation space into a *cis* side and a *trans* side. The thickness of the membrane is one layer, i.e., the membrane occupies one lattice layer, as shown in Fig. 1. Both the polymers and the NPs cannot penetrate the membrane. A small noninteracting pore with size 1×3 lattices is located at the center of the membrane, through which the polymers can escape from the *cis* side and enter the *trans* side. But NPs are bigger than the pore, therefore they only stay at the *trans* side. Periodic boundary conditions are considered in

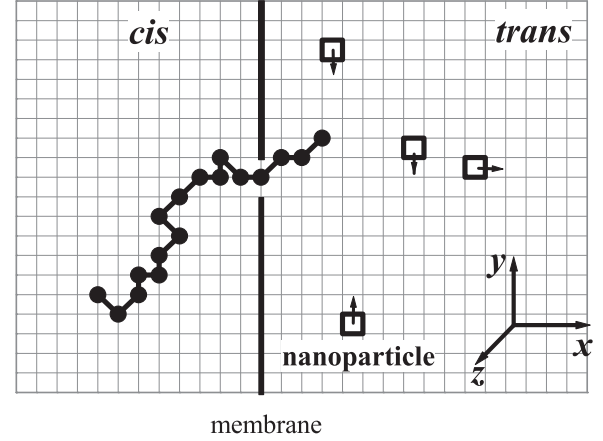


FIG. 1. A two-dimensional side view of the schematic representation of polymer translocation through a nanopore in the membrane at $x = 0$. Attractive NPs distributed at the *trans* side move randomly with mobility V . There is no NP at the *cis* side.

the y and z directions, whereas the free boundary condition is applied in the x direction.

The NP concentration, ϕ_t , is defined as the fraction of NP sites at the *trans* side:

$$\phi_t = \frac{8n}{V_t}. \quad (1)$$

Here, n and V_t are the number of NPs and total lattice sites at the *trans* side, and the factor 8 is due to the fact that one NP occupies eight lattice sites. NPs are also self-avoiding, that is, no site can be occupied by two or more NPs simultaneously.

Polymers and NPs cannot overlap during the whole simulation run. Only if a polymer segment is located at the nearest-neighbor (NN) site of the NP do we assign an interaction energy E for the polymer-NP pair. In this paper, $k_B T$ is used as the unit of energy, so the reduced interaction strength is denoted as $\varepsilon = -E/k_B T$. Here, k_B is Boltzmann's constant and T is the temperature. Therefore, a positive ε indicates the attraction between polymers and NPs.

The dynamics of a polymer chain is achieved through the random bond fluctuation method [45]. We randomly choose a segment of polymers and move it to one of its six NN sites. An allowed NN site should satisfy the following three conditions: (i) original empty, (ii) without bond crossing, and (iii) bond length being allowed if the chosen segment moves there. If the new site does not satisfy the three conditions, the trial move is rejected. Otherwise the trial move will be accepted or rejected according to the METROPOLIS algorithm. That is, the move is accepted with the probability $p = \min[1, \exp(-\Delta E/k_B T)]$, where ΔE is the energy shift due to the trial move. The time unit is one Monte Carlo step (MCS), during which N trial moves are tried. The time unit MCS can be scaled to a real-time unit. To accelerate the translocation of polymers, a chemical potential difference $\Delta\mu$ (in the unit of $k_B T$) between the *cis* side and the *trans* side is considered. In this case, the polymer will gain energy $\Delta\mu$ when a segment runs from the *cis* side into the *trans* side. $\Delta\mu$ serves as a driving force to pull the polymer through the pore.

Like polymers, NPs also move one lattice unit in each trial move. NPs could have a different mobility from the polymer segment due to different masses. The NP mobility is set as V , which is in inverse proportion to the mass of NPs. If $V < 1$, each NP has a probability V to move one lattice unit in one MCS, whereas if $V \geq 1$, each NP moves V times in one MCS. For every trial move, we randomly choose one NP and move it one lattice unit in one of six directions. Similarly, this trial move will be accepted with the probability $p = \min[1, \exp(-\Delta E/k_B T)]$ if the move does not violate the EV.

At the beginning of every simulation, the pore at the center of the membrane at $x = 0$ is closed and NPs are placed randomly at the *trans* side without overlap. To reduce the simulation time, the head segment of the polymer is fixed at a site near the pore, while other segments are generated in sequence in the *cis* space. We then equilibrate the system by a long-time random motion of the polymer except the head segment. The equilibrium time scale is set as $N^{2.2}$, a relaxation time scale for the SAW polymer. The equilibrium conformation $\{s_0\}$ is recorded in the simulation. Afterward, we open the pore and release the head segment of the polymer to allow the polymer to translocate through the pore. However, because of the energy barrier and the thermal noise, the polymer may be drawn back into the *cis* side again even if a few monomers enter the *trans* side. This constitutes an ‘‘attempted’’ translocation. To save simulation time, we reset the equilibrium conformation $\{s_0\}$ if the whole polymer is drawn back. As we focus on the translocation dynamics of polymers, such a treatment does not influence the simulation of the translocation dynamics as well as the determination of the translocation time. Finally, there is a ‘‘successful’’ translocation

during which the polymer translocates continuously through the pore without a complete withdrawal. The definition of the translocation time τ is the time duration for the final successful polymer translocating, which is the same as that defined in experiments [4,9]. After we obtain a ‘‘successful’’ translocation, we then record the simulation results and start the next independent simulation run.

The size of the simulation system is $121 \times 40 \times 40$ for the translocation of polymer. The membrane at $x = 0$ is placed at the middle of the system. The thickness of the membrane is 1. The sizes of the *cis* side and the *trans* side are $60 \times 40 \times 40$. Our results are averaged over 2000 independent runs.

III. SIMULATION RESULTS AND DISCUSSIONS

A. Polymer translocation

We first investigate the effect of dynamic interacting NPs on the mean translocation time $\langle \tau \rangle$ of polymers. Our simulations are carried out for different polymer lengths, NP concentrations, NP mobilities, and chemical potential differences. The NP concentration is varied from low, $\phi_t = 0.01$, to high, $\phi_t = 0.15$. The concentration $\phi_t = 0.15$ was found to be a high value for the static case [40]. Therefore, a chemical potential difference $\Delta\mu < 0$, which serves as a driving force, is often used to accelerate the translocation and thus to decrease the simulation time. Figure 2 presents $\langle \tau \rangle$ as a function of ε for several simulation parameters: polymer length N , chemical potential difference $\Delta\mu$, NP concentration ϕ_t , and mobility V . For all cases except those at large $|\Delta\mu|$, the dependence of $\langle \tau \rangle$ on ε is similar: with an increase in the attractive strength ε , $\langle \tau \rangle$ decreases slowly at weak attractive interactions but increases fast at strong attractive interactions. We find that

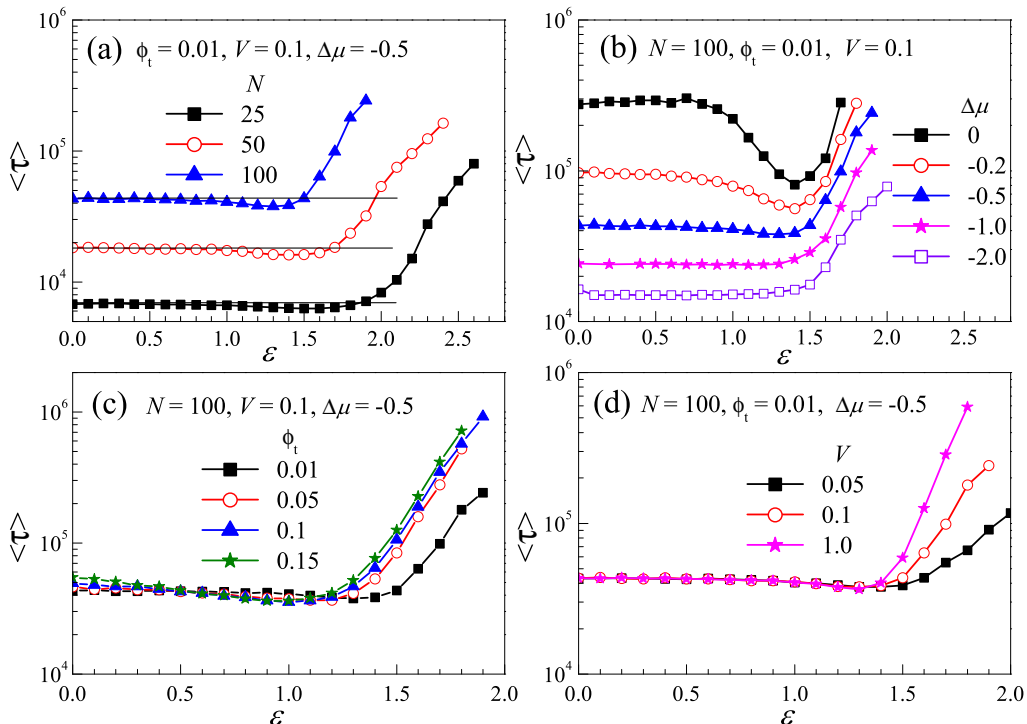


FIG. 2. (Color online) The mean translocation time $\langle \tau \rangle$ as a function of polymer-NP interaction ε for different parameters: polymer length N (a), chemical potential difference $\Delta\mu$ (b), NP concentration ϕ_t (c), and NP mobility V (d). Solid lines in (a) are parallel to the x axis.

such behavior becomes more obvious at larger N , therefore we use $N = 100$ in the simulations for other parameters. The behavior is obvious at $\Delta\mu = 0$, but it almost disappears at strong driving $\Delta\mu = -1$ and -2 . Because more simulation time is required at smaller $|\Delta\mu|$, most of our simulations are carried out at $\Delta\mu = -0.5$. Moreover, the behavior is roughly independent of the NP concentration and NP mobility.

We then define an optimal interaction ε^* at which $\langle\tau\rangle$ is minimal. The optimal interaction ε^* may separate a weak attraction regime and a strong one. We find that the value ε^* decreases with the increase in the polymer length N , as shown in Fig. 2(a), and the NP concentration ϕ_t , as shown in Fig. 2(c). But it is roughly independent of the chemical potential difference $\Delta\mu$, as shown in Fig. 2(b), and the NP mobility V , as shown in Fig. 2(d).

The behavior of $\langle\tau\rangle$ shown in Fig. 2 indicates that weak attractive NPs help polymers to translocate into the *trans* side, but strong attractive NPs prevent polymers from translocating into the *trans* side. This implies, therefore, that NPs may have two opposite effects on the translocation of polymers. The attractive interaction between polymers and NPs provides an intrinsic driving force to pull the polymers by lowering the free energy when the polymers enter the *trans* side. Thus the attractive interaction can accelerate polymer translocation. But the translocation is quite fast at short N or big $|\Delta\mu|$ [Figs. 2(a) and 2(b)]. In this case, the effect of NPs is suppressed and therefore the decrease in the translocation time is not obvious. On the other hand, the attractive interaction will result in the contact of polymers with NPs, and thus a decrease in the diffusion rate of the polymers. We find that $\langle\tau\rangle$ increases sharply at large ε as NPs will significantly slow down polymer translocation at strong attraction. Because of the competition between these two effects, there exists an optimal interaction ε^* at which the polymer chain translocates the most quickly. Such behavior is similar to that of polymer translocation in the system with static NPs [40]. We also find that the value of ε^* decreases with the increase in the NP concentration ϕ_t [Fig. 2(c)], which is also similar to the case of static NPs [40].

The main work in this subsection is to find out the effect of NP mobility on the translocation of polymers. Toward that end, we have simulated the dependence of mean translocation time $\langle\tau\rangle$ on the NP mobility V . The results are presented in Fig. 2(d). We find that $\langle\tau\rangle$ is roughly independent of V when ε is close to 0, and it decreases slightly with V at very weak attractions, $\varepsilon \ll \varepsilon^*$. However, we find that $\langle\tau\rangle$ is strongly dependent on V at ε near or larger than ε^* .

Figure 3 shows the relation between the mean translocation time $\langle\tau\rangle$ and the NP mobility V for different NP concentrations ϕ_t at relatively strong attractions $\varepsilon > \varepsilon^*$. We find that $\langle\tau\rangle$ increases and then decreases with the increase in V . The value V^* at which $\langle\tau\rangle$ is maximal shifts to small value when ϕ_t or ε increases. It is interesting to find that, near V^* , the dependence of $\langle\tau\rangle$ on V can be expressed by power-law relations:

$$\langle\tau\rangle \sim V^{\eta_1} \quad (2)$$

at $V < V^*$ and

$$\langle\tau\rangle \sim V^{-\eta_2} \quad (3)$$

at $V > V^*$. Both the exponents η_1 and η_2 increase with the increase in ϕ_t and ε . At present, the underlying physics for these

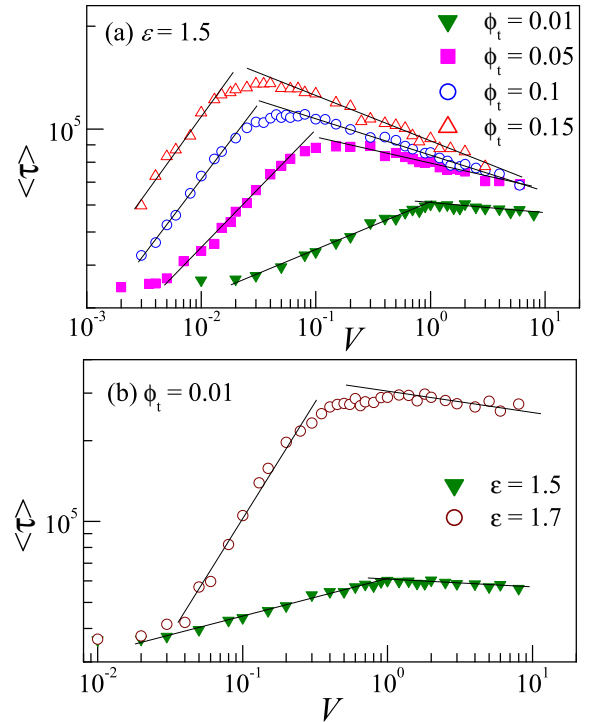


FIG. 3. (Color online) Log-log plot of the mean translocation time $\langle\tau\rangle$ as a function of the NP mobility V for polymers at different NP concentrations ϕ_t and at $\varepsilon = 1.5$ (a) and for polymers at different polymer-NP attractions ε and at $\phi_t = 0.01$ (b). Other parameters are polymer length $N = 100$ and chemical potential difference $\Delta\mu = -0.5$. Solid lines are guides for the eyes.

behaviors is not clear. However, the dynamics of NPs seems to provide an additional drag force at small V and an additional driving force at large V . It is well known that the dependence of τ on the driving force is a power-law relation [46]. If V tends to 0, the translocation time $\langle\tau\rangle$ will plateau to a constant value (independent of V), as shown in Fig. 3.

Our simulation results show that the effect of NP mobility on the translocation of polymers is dependent on the polymer-NP interaction. This is because the free energy of polymers is strongly dependent on the polymer-NP interaction [39–41]. On the other hand, the translocation time is also dependent on the diffusion rate of polymers. Therefore, at the same polymer-NP interaction, the effect of NPs relies mainly on the number of NPs contacting the polymers, N_c , and the duration of contact time, τ_c . Our results will show that, at neutral or weak attractions, N_c and τ_c are close to 0 and are roughly independent of the motion of NPs. Thus the translocation time is roughly independent of V at $\varepsilon < \varepsilon^*$, as shown in Fig. 2(d). But at strong attraction (ε close to or larger than ε^*), the situation becomes complicated. The contact of NP with polymers will decrease the energy of the system, which will decrease $\langle\tau\rangle$. In contrast, it will also reduce the possible number of polymer conformations and decrease the diffusion rate of polymers due to the EV effect, which will increase $\langle\tau\rangle$. Similarly, the mobility of NPs also shows two competitive effects. Our results will show that the increase in V will increase the number of contacted NPs and therefore reduce the diffusion rate of polymers. This effect will increase $\langle\tau\rangle$. But large V could also increase the

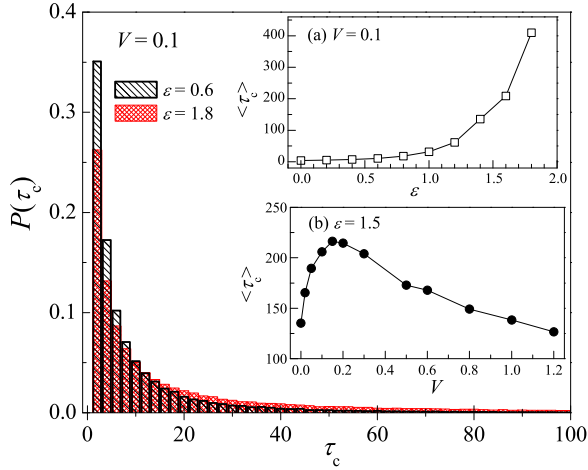


FIG. 4. (Color online) The distribution probability of contact time $P(\tau_c)$ for weak polymer-NP attraction $\varepsilon = 0.6$ and strong attraction $\varepsilon = 1.8$. Insets: the dependence of mean contact time $\langle \tau_c \rangle$ on the polymer-NP interaction at $V = 0.1$ (a) and on the NP mobility at $\varepsilon = 1.5$ (b). Parameters: polymer length $N = 100$, chemical potential difference $\Delta\mu = -0.5$, and NP concentration at the *trans* side $\phi_t = 0.01$.

probability of NPs diffusing away from the polymers or decrease the contact time τ_c . This will provide more empty NN sites for the polymers and reduce the effects of EV. Therefore, $\langle \tau \rangle$ could decrease with the increase in V . As a result, we observe a peak of $\langle \tau \rangle$ at moderate V as shown in Fig. 3. In short, the results shown in Figs. 2 and 3 clearly indicate that both ε and V have two opposite effects to accelerate or slow down the translocation.

We then simulate the effects of the polymer-NP interaction on the distribution of the contact time τ_c of NPs. Figure 4 presents the distribution probabilities $P(\tau_c)$ for weak and strong attractive interactions. The probability $P(\tau_c)$ at large τ_c for the strong attraction $\varepsilon = 1.8$ is obviously larger than that for the weak attraction $\varepsilon = 0.6$, which means that NPs will adhere to polymers for a longer time at a stronger attraction. We have calculated the mean contact time $\langle \tau_c \rangle$ at different attraction strengths ε and NP mobilities V as presented in the insets of Fig. 4. We simply find that $\langle \tau_c \rangle$ increases with the increase in ε . But $\langle \tau_c \rangle$ shows a maximum with the increase of V , a profile similar to the translocation time shown in Fig. 3. The results show that the contact between polymers and NPs is an important factor in explaining the behavior of polymer translocation.

In addition to the number of polymers contacting NPs, N_c , we have also calculated the number of polymer-NP pairs, N_p . If any of the NN sites of a NP is occupied by polymers, the NP is identified as a polymer-contacted NP, while a polymer and a NP located at a NN site constitute a polymer-NP pair. A polymer-contacted NP may have more than one polymer-NP pair. Therefore, we have $N_p \geq N_c$.

The inset of Fig. 5(a) presents the variation of N_c/m with the elapsed time normalized by translocation time in the whole translocation process for the case of strong attractive interaction $\varepsilon = 1.5$. Here m is the number of translocated segments at the *trans* side. We find that N_c/m increases with V . The results clearly show that it is easy for a dynamic NP

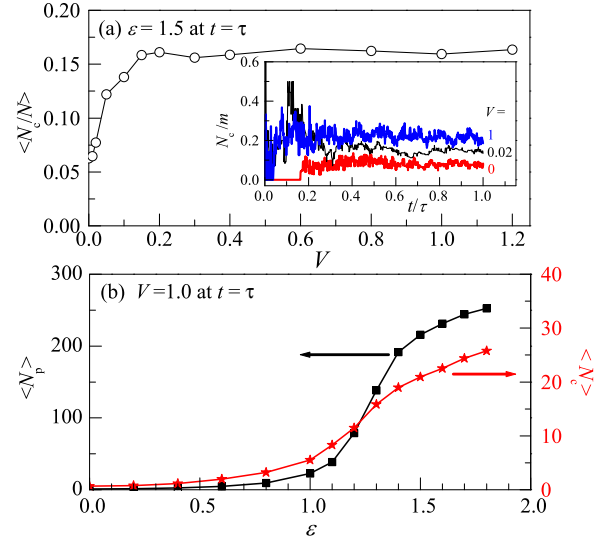


FIG. 5. (Color online) (a) Mean number of polymer-contacted NPs $\langle N_c/N \rangle$ vs the mobility V at attractive strength $\varepsilon = 1.5$. Inset: the number of polymer-contacted NPs N_c varies with time t/τ during the translocation process at different NP mobilities $V = 0, 0.02$, and 1.0 (from bottom to top). (b) Variation of the mean number of polymer-NP pairs $\langle N_p \rangle$ and the mean number of polymer-contacted NPs $\langle N_c \rangle$ at the end of the polymer translocation with the interaction ε . Other parameters: polymer length $N = 100$, chemical potential difference $\Delta\mu = -0.5$, and NP concentration $\phi_t = 0.01$.

to come in contact with a polymer. This will attract polymers but decrease the diffusion of polymers. Figure 5(a) shows the mean value $\langle N_c/N \rangle$ at the end of the translocation, i.e., at $t = \tau$. $\langle N_c/N \rangle$ increases fast with V at first, and then reaches a saturated value. Although a higher contact number (larger $\langle N_c/N \rangle$) is expected at larger V , the decrease of the translocation time τ at large V (Fig. 3) would probably decrease the value of $\langle N_c/N \rangle$. The two competitive effects might result in a saturation in $\langle N_c/N \rangle$ at large V , as shown in Fig. 5(a).

We have calculated the average number of polymer-NP pairs $\langle N_p \rangle$ and the average number of polymer-contacted NPs $\langle N_c \rangle$ at the end of polymer translocation, i.e., at $t = \tau$. Figure 5(b) shows the dependence of $\langle N_p \rangle$ and $\langle N_c \rangle$ at $t = \tau$ on the polymer-NP interaction ε . Both $\langle N_p \rangle$ and $\langle N_c \rangle$ are very small at weak attractions, $\varepsilon < 1.0$. That is, NPs are not adsorbed on the polymer at weak attractions. However, some NPs adhere to the polymers at strong attractive interactions, resulting in an increase of $\langle N_p \rangle$ and $\langle N_c \rangle$. We have simulated the results for different NP mobilities, and we find similar behavior for both $\langle N_p \rangle$ and $\langle N_c \rangle$.

The translocation of polymers depends significantly on the free-energy landscape [14,17]. In the present case, the free-energy landscape is related to the interaction between polymers and NPs. For simplification, we use the average contact energy $-\langle N_p \rangle \varepsilon$ at $t = \tau$ to describe the interaction between polymers and NPs. Figure 6 shows the dependence of the mean translocation time $\langle \tau \rangle$ on $\langle N_p \rangle \varepsilon$ for different NP mobilities and for two chemical potential differences $\Delta\mu = 0$ and -0.5 . Although the NP mobility influences the number of NPs near the polymer, it is interesting to see that the

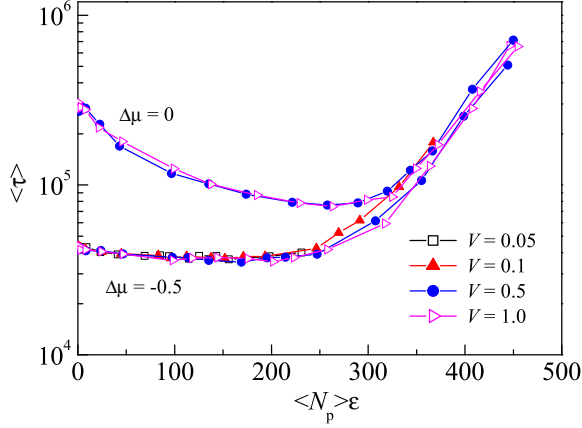


FIG. 6. (Color online) The dependence of the mean translocation time $\langle \tau \rangle$ on average contact energy $\langle N_p \rangle \varepsilon$ for different NP mobilities $V = 0.05, 0.1, 0.5,$ and 1.0 at $\Delta\mu = 0$ and -0.5 . Here polymer length $N = 100$ and NP concentration $\phi_t = 0.01$.

translocation time can be roughly determined by the average contact energy $-\langle N_p \rangle \varepsilon$ at $t = \tau$. Similar to Fig. 2(d), there is a minimum of $\langle \tau \rangle$ for $\Delta\mu = 0$ and -0.5 , and the place of the minimum is roughly independent of V . An interesting phenomenon is that, at large $\langle N_p \rangle \varepsilon$, $\langle \tau \rangle$ is roughly independent of $\Delta\mu$, indicating that large attraction energy could dominate the driving force $\Delta\mu$ in the polymer translocation. The results clearly show that the interaction between NPs and polymers plays an important role in the polymer translocation. However, as the translocation of polymers is also dependent on other factors, such as polymer length, driving force, and diffusion rate, we find that only the data of Fig. 2(d) can be overlapped by introducing $\langle N_p \rangle \varepsilon$.

During the process of a linear polymer translocation through the nanopore, the linear polymer can be treated as two connected end-grafted polymers [12]. Because of the loss of the configuration number when the polymer enters the nanopore, there is a free-energy barrier for the translocation. Therefore, it is difficult for the polymer to enter the pore. But the polymer enters the *trans* side fast when it overcomes the free-energy barrier. Thus the translocation process is an off-equilibrium process even at $\Delta\mu = 0$ [19]. The just translocated polymer at $t = \tau$ can be regarded as an end-grafted polymer, but the conformational size is obviously squeezed [47]. It was found that the conformational size of the just translocated polymer is smaller than that of an equilibrium end-grafted polymer [47,48].

The presence of dynamic NPs at the *trans* side also influences the conformational size of the just translocated polymer. The conformational size of the polymer can be described by the mean-square end-to-end distance $\langle R^2 \rangle$ and the mean-square radius of gyration $\langle R_G^2 \rangle$. We have calculated $\langle R^2 \rangle$ and $\langle R_G^2 \rangle$ for the polymer at $t = \tau$. Figure 7(a) shows the variation of $\langle R^2 \rangle$ and $\langle R_G^2 \rangle$ on the polymer-NP interaction ε . We find that the size of the polymer decreases with an increase in ε , confirming that polymers becomes more and more compact with an increase in the attractive interaction. The reason for this is that polymer segments may be adsorbed on NPs firmly, and it is hard for them to diffuse away at strong

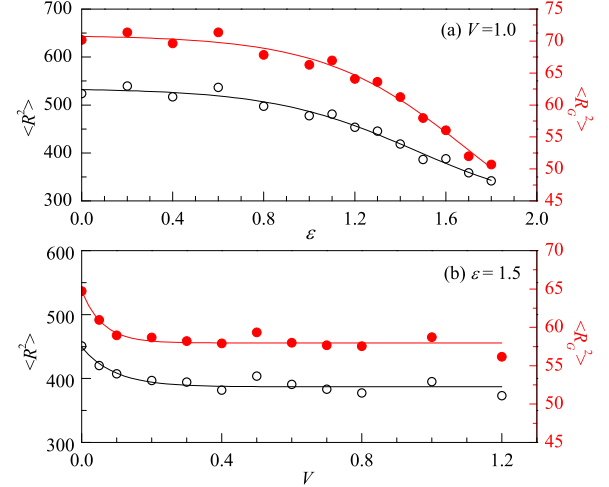


FIG. 7. (Color online) The dependence of the mean-square end-to-end distance $\langle R^2 \rangle$ (black open circles) and the mean-square radius of gyration $\langle R_G^2 \rangle$ (red solid circles) on the polymer-NP interaction ε at $V = 1$ (a) and on the NP mobility V at $\varepsilon = 1.5$ (b). Polymer length is $N = 100$, chemical potential difference $\Delta\mu = -0.5$, and NP concentration $\phi_t = 0.01$. Solid lines are guides for the eyes.

interactions. Figure 7(b) presents the variation of $\langle R^2 \rangle$ and $\langle R_G^2 \rangle$ on the NP mobility V at strong attraction $\varepsilon = 1.5$. We find that the size of the polymers decreases with an increase in V obviously at small V , but it is almost saturated at large V . At small V , the conformation of the chain is extended because the polymer is adsorbed to dispersed NPs that will stretch the polymer chain, as in the situation of polymers in an environment with static NPs [49]. When V increases, adsorbed NPs move toward the polymers and the adsorbed NPs serve as an adsorbing core, therefore the conformation of polymers becomes compact.

B. Dynamics of polymers in media with NPs

The behavior of polymer translocation is strongly related to the conformation and diffusion properties of polymers [46]. To better understand the translocation behaviors of polymers entering crowded media observed in the previous subsection, we study the conformation and diffusion properties of polymer chains in crowded media filled with dynamic NPs. Our simulations are carried out in a box of size $80 \times 80 \times 80$ with periodic boundary conditions in all three directions. The polymer length is $N = 100$ while the NP concentration is mostly set as $\phi = 0.01$. The statistical results are averaged over 2000 independent runs.

The conformation property of a polymer chain can be viewed from the statistical size and the instantaneous shape of the polymers. The instantaneous shape is not spherical even in solution. Rather, it is usually described by the mean asphericity parameter $\langle A \rangle$ defined as [50,51]

$$\langle A \rangle = \left\langle \frac{\sum_{i>j}^3 (L_i^2 - L_j^2)}{2 \left(\sum_{i=1}^3 L_i^2 \right)^2} \right\rangle \quad (4)$$

in three dimensions, where L_1^2 , L_2^2 , and L_3^2 are three eigenvalues of the radius of gyration tensor. The asphericity

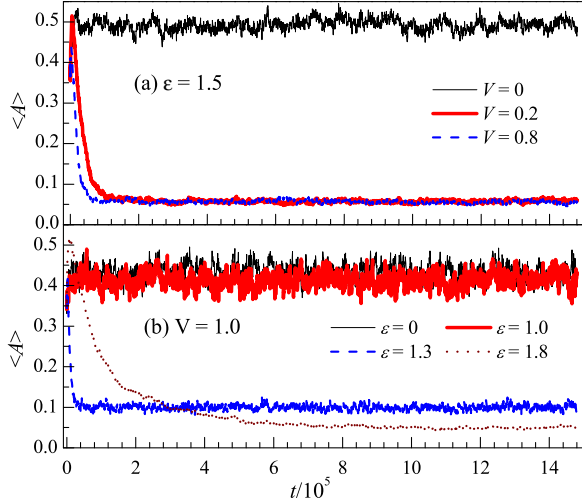


FIG. 8. (Color online) (a) The dependence of asphericity parameter $\langle A \rangle$ on relaxation time t at different NP mobilities: $V = 0$ (thin solid black line), 0.2 (thick solid red line), and 0.8 (dashed blue line). Here the polymer-NP interaction is $\epsilon = 1.5$. (b) Evolution of $\langle A \rangle$ at different polymer-NP interactions: $\epsilon = 0$ (thin solid black line), 1.0 (thick solid red line), 1.3 (dashed blue line), and 1.8 (dotted purple line). Here the NP mobility is $V = 1$. Other parameters: polymer length $N = 100$ and NP concentration $\phi = 0.01$.

parameter $\langle A \rangle$ ranges from 0 for 3D spherically symmetric conformations, 0.25 for 2D circular-shape conformations, and 1 for long rod-shaped ones. It was found that $\langle A \rangle$ was about 0.391 for a linear random-walk (RW) chain and about 0.431 for a linear SAW chain [50].

Figure 8 presents the evolution of the mean asphericity parameter $\langle A \rangle$ at different NP mobilities and at different polymer-NP interactions. The variation of the statistical sizes, $\langle R^2 \rangle$ and $\langle R_G^2 \rangle$, is not presented since they show similar behavior to that of $\langle A \rangle$. This is in agreement with the positive correlation between shape and size for a linear polymer [52]. Here the starting point $t = 0$ is at the moment we put NPs and polymers into the system. For the static NP case with $V = 0$, $\langle A \rangle$ is large and almost independent of time, indicating that the conformation is always a random coil in the system. For the case of dynamic NPs, the polymer chain adjusts its conformation quickly, as shown in Fig. 8(a). $\langle A \rangle$ decreases to almost 0, indicating that the polymers change from a random coil to a spherelike conformation. Figure 8(b) shows that the conformation of the polymer chain does change with time, and $\langle A \rangle$ maintains a high value at weak attractions $\epsilon = 0$ and 1.0, which means only a few NPs come in contact with polymers under these conditions. In contrast, $\langle A \rangle$ drops to a low value at strong attraction $\epsilon = 1.3$ and 1.8, which means that some adsorbed NPs pull polymers together and make their conformation compact. Therefore, polymer segments move slowly at strong attraction, and polymers spend much more time reaching equilibrium at stronger attraction.

After equilibrating the polymer chain, we calculate the mean asphericity parameter $\langle A \rangle$, the mean number of polymer-NP pairs $\langle N_p \rangle$, and the mean number of polymers contacting NPs $\langle N_c \rangle$. The results at different polymer-NP interactions are presented in Fig. 9. For weak attraction $\epsilon < 1.0$, $\langle A \rangle$ is large

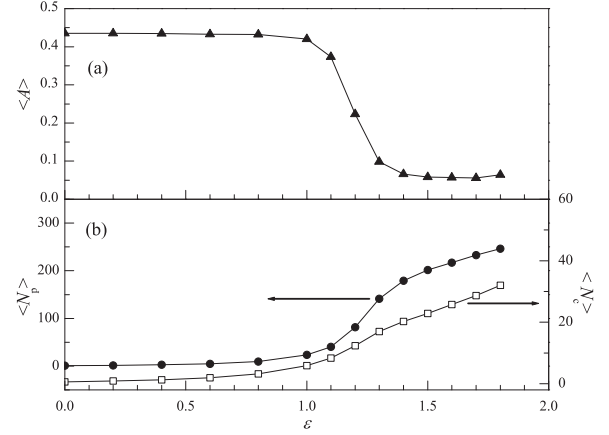


FIG. 9. The dependence of mean asphericity parameter $\langle A \rangle$ (a) and mean number of polymer-NP pairs $\langle N_p \rangle$ (solid circle) and mean number of polymer-contacted NPs $\langle N_c \rangle$ (open square) (b) on polymer-NP interaction ϵ for polymers in a crowded environment. Parameters: polymer length $N = 100$, NP concentration $\phi = 0.01$, and NP mobility $V = 1$.

with a value about 0.43 [Fig. 9(a)], whereas $\langle N_p \rangle$ and $\langle N_c \rangle$ are small [Fig. 9(b)], which means that the conformation of polymers is a random coil and the polymers only come into contact with a small number of NPs. For strong attraction $\epsilon > 1.0$, $\langle A \rangle$ decreases rapidly to below 0.1, whereas $\langle N_p \rangle$ and $\langle N_c \rangle$ increase to high values. It is clear that NPs attract polymers and pull them together. Polymers behave like a compact sphere in this case.

The diffusion property of a polymer chain in the media with dynamic NPs is also investigated. The diffusion of polymers can be described by the time dependence of the mean-square displacement (MSD) of the mass center of the polymers, which is defined as

$$\langle \Delta r^2 \rangle \equiv \langle |\vec{r}_{\text{cm}}(t) - \vec{r}_{\text{cm}}(0)|^2 \rangle. \quad (5)$$

Here, $\vec{r}_{\text{cm}}(t)$ is the position vector of the center of mass of the chain at time t . If the diffusion is normal, i.e.,

$$\langle \Delta r^2 \rangle \sim t, \quad (6)$$

we can define the diffusion constant D as $D = \langle \Delta r^2(t) \rangle / 6t$ for large t , whereas for subnormal diffusion,

$$\langle \Delta r^2 \rangle \sim t^b, \quad (7)$$

with $b < 1$, the diffusion becomes slow as a caged-particle motion [53,54].

Figure 10 shows the evolution of $\langle \Delta r^2 \rangle$ at different NP concentrations and polymer-NP interactions at $V = 0.1$. For polymers in the media with dynamic NPs, the diffusion of polymers is always normal at a long time scale for all the cases. This is absolutely different from the diffusion property of polymers in an environment with static NPs where subnormal diffusion was observed [40]. At small ϵ , $\langle \Delta r^2 \rangle - t$ curves almost overlap, which means that the diffusion constant D is roughly independent of ϵ for weak interactions. However, D decreases obviously at strong attractive interaction due to the adsorption of NPs on the polymer. At $\epsilon = 1.2$ and 1.5, the diffusion is subnormal at a short time scale, a situation

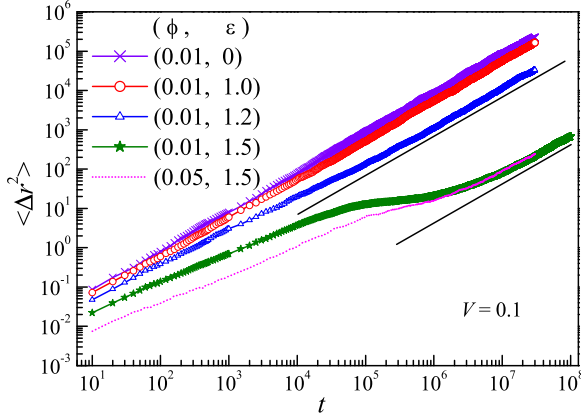


FIG. 10. (Color online) Log-log plot of the mean-square displacement of the center of mass $\langle \Delta r^2 \rangle$ vs simulation time t at different NP concentrations ϕ and polymer-NP interactions ε . Other parameters: polymer length $N = 100$ and NP mobility $V = 0.1$. The straight lines with slope 1.0 indicate the normal diffusion of polymers.

analogous to that of polymers or particles moving within a cage [55]. In the present model, the cage is formed due to the adsorption of polymers on NPs. However, polymers can move across the cages and the diffusion becomes normal with $b = 1$ at a long time scale. The plateau at an intermediate time scale indicates the duration for the polymer moving across cages. By comparing two diffusion curves for $\varepsilon = 1.2$ and 1.5 for the same ϕ and ε in Fig. 10, we find that the subnormal diffusion at a short time scale is more obvious at $\varepsilon = 1.5$ because the NP cage becomes stronger with the increase in ε . For the same reason, the plateau becomes wider at larger ε .

However, we find that the diffusion on ϕ is dependent on the polymer-NP attraction ε . At weak polymer-NP attraction $\varepsilon < \varepsilon^*$, the diffusion is normal at different ϕ 's, but the diffusion constant decreases with the increase in ϕ . The results are not presented in this paper due to their simplicity. In this case, NPs hamper the diffusion of polymers, and such a decrease in the diffusion constant becomes obvious with the increase in ε . In contrast, at strong attraction $\varepsilon = 1.5$, we find that the diffusion becomes slow but the plateau becomes narrow with the increase in ϕ , as shown in Fig. 10. At higher ϕ , it is easy to form smaller cages, and therefore the short time-scale diffusion is slow. However, polymers take a shorter amount of time to travel across a small cage, therefore the plateau becomes narrower. Although the diffusion rate decreases with the increase in ϕ at the short time scale, it is interesting to find that the diffusion rate is roughly independent of ϕ for the dynamic NPs at a long time scale.

Finally, we have investigated the influence of NP mobility on the diffusion of polymers. For weak attractive NPs $\varepsilon < \varepsilon^*$, normal diffusion is always observed for polymers in the media with dynamic NPs $V = 0.1$ and 0.5. Again, the results are not presented in this paper due to their simplicity. At $\varepsilon = 0$, we find that the diffusion constant D is roughly independent of V . With the increase in ε , however, we find that the diffusion constant D increases with V . In this case, the weak attractive dynamic NPs enhance the dynamics of polymers.

The situation of polymers in the presence of strong attractive NPs is complicated and interesting. Figure 11

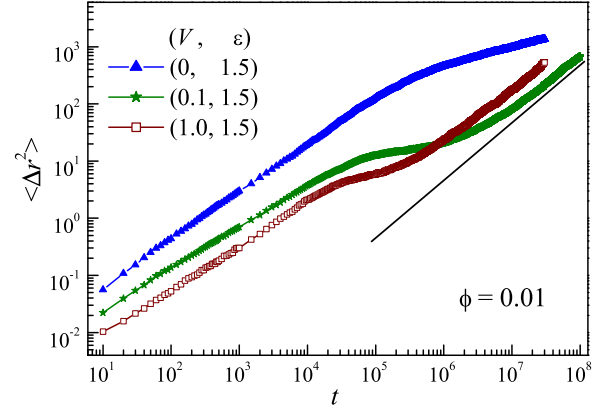


FIG. 11. (Color online) Log-log plot of the mean-square displacement of the center of mass $\langle \Delta r^2 \rangle$ vs simulation time t at different NP mobilities V . Other parameters: polymer length $N = 100$ and polymer-NP interactions $\varepsilon = 1.5$. The straight line with slope 1.0 indicates the normal diffusion of polymers.

shows the evolution of $\langle \Delta r^2 \rangle$ for different NP mobilities at polymer-NP interaction $\varepsilon = 1.5$. At $V = 0$, the plateau of diffusion is very wide, therefore it is difficult to show long time behavior for this case. The dynamics of polymers shows two different time regions. At a short-time-scale region, the diffusion is subnormal and the diffusion decreases with the increase in V , indicating that the adsorption of NPs retards the diffusion of polymers. At a long time scale, the diffusion is normal and the diffusion constant D increases with V , which is analogous to the weak attraction case, therefore the dynamic NPs accelerate the diffusion of polymers. It is easy to understand that the plateau of diffusion becomes shorter with the increase in V , because dynamic NPs will break the cage by themselves.

As the translocation time τ shown in Figs. 2 and 3 varies obviously with the polymer-NP interaction, NP concentration, and NP mobility, the value τ can be at the short time scale or at the long time scale of diffusion shown in Figs. 10 and 11. Nevertheless, the diffusion of polymers in both time scales is strongly dependent on these parameters. Therefore, the translocation of polymers in the crowded media would be strongly related to the diffusion of polymers.

In short, the conformation and diffusion properties of a polymer chain are strongly influenced by the dynamics of NPs and polymer-NP interaction. The results are in agreement with the new behaviors of polymers translocating into a crowded environment with dynamic NPs.

IV. CONCLUSION

In this paper, we have studied the translocation of a self-avoiding bond fluctuation model polymer through a small pore into a crowded media with dynamic nanoparticles (NPs) at the *trans* side. The translocation time is dependent on the polymer-NP interaction and the NP mobility as well. The dynamic NP at the *trans* side can raise the free-energy landscape due to the excluded volume effect and thus hinder the polymer translocation, therefore the translocation time increases compared with the case of free translocation in the

absence of NPs. On the other hand, the attractive interaction between polymers and NPs can provide a driving force on the polymers and accelerate the translocation process by lowering the free energy, whereas strong attraction is a disadvantage to the translocation of polymers because of the strong contact between NPs and polymers. The contact time increases with the increase in polymer-NP attraction, but it is dependent on the NP mobility. The dynamics of NPs affects the translocation of polymers by influencing the contact between NPs and polymers. With the increase in NP mobility, we observe a power-law increase of translocation time at small mobility and a power-law decrease at large mobility.

The diffusion properties of a polymer chain in the crowded media is also affected by the polymer-NP interaction and the NP mobility, resulting in the new behaviors of polymer translocating into the crowded environment with dynamic NPs. We find that the diffusion of polymers in the presence of dynamic NPs is always normal at a long time scale. The diffusion constant decreases obviously at strong polymer-NP attraction but increases with NP mobility. Moreover, our results

show that the effect of attractive NPs on the dynamics of polymers is dependent on the time scale at strong polymer-NP attraction. We find that the diffusion decreases with the increase in NP mobility at a short time scale, but it increases with the mobility at a long time scale.

Therefore, the effect of attractive mobile NPs on the translocation of polymers can be summarized as follows: (i) there is an excluded volume effect that decreases the polymer entropy, (ii) it provides a driving force on polymers by decreasing the system energy, and (iii) it changes the diffusion property of polymers by influencing the contact between NPs and polymers.

ACKNOWLEDGMENTS

This work was supported by the National Natural Science Foundation of China under Grants No. 21174132, No. 11374255, and No. 11447184. W.P.C. gratefully acknowledges the financial support from Zhejiang Provincial Natural Science Foundation of China under Grant No. LQ14A040001.

-
- [1] B. Alberts and D. Bray, *Molecular Biology of the Cell* (Garland, New York, 1994).
- [2] B. Alberts, A. Johnson, J. Lewis, M. Raff, K. Roberts, and P. Walter, *Molecular Biology of the Cell* (Garland, New York, 2002).
- [3] M. Akeson, D. Branton, J. J. Kasianowicz, E. Brandin, and D. W. Deamer, *Biophys. J.* **77**, 3227 (1999).
- [4] J. J. Kasianowicz, E. Brandin, D. Branton, and D. W. Deamer, *Proc. Natl. Acad. Sci. USA* **93**, 13770 (1996).
- [5] J. Han, S. W. Turner, and H. G. Craighead, *Phys. Rev. Lett.* **83**, 1688 (1999).
- [6] D.-C. Chang, *Guide to Electroporation and Electrofusion* (Academic, New York, 1992).
- [7] W. W. Yan, J. J. Kirkland, and D. D. Bly, *Modern Size-exclusion Liquid Chromatography* (Wiley, New York, 1992).
- [8] S. E. Henrickson, M. Misakian, B. Robertson, and J. J. Kasianowicz, *Phys. Rev. Lett.* **85**, 3057 (2000).
- [9] A. Meller, L. Nivon, and D. Branton, *Phys. Rev. Lett.* **86**, 3435 (2001).
- [10] A. Mattozzi, B. Neway, M. S. Hedenqvist, and U. W. Gedde, *Polymer* **46**, 929 (2005).
- [11] W. Sung and P. J. Park, *Phys. Rev. Lett.* **77**, 783 (1996).
- [12] M. Muthukumar, *J. Chem. Phys.* **111**, 10371 (1999).
- [13] R. E. Boehm, *Macromolecules* **32**, 7645 (1999).
- [14] K. L. Sebastian and A. K. R. Paul, *Phys. Rev. E* **62**, 927 (2000).
- [15] M. Muthukumar, *J. Chem. Phys.* **118**, 5174 (2003).
- [16] E. Slonkina and A. B. Kolomeisky, *J. Chem. Phys.* **118**, 7112 (2003).
- [17] M. Muthukumar, *Phys. Rev. Lett.* **86**, 3188 (2001).
- [18] S. S. Chern, A. E. Cardenas, and R. D. Coalson, *J. Chem. Phys.* **115**, 7772 (2001).
- [19] J. Chuang, Y. Kantor, and M. Kardar, *Phys. Rev. E* **65**, 011802 (2001).
- [20] P. Tian and G. D. Smith, *J. Chem. Phys.* **119**, 11475 (2003).
- [21] C. M. Chen, *Physica A* **350**, 95 (2005).
- [22] M. B. Luo, *Polymer* **46**, 5730 (2005).
- [23] K. F. Luo, T. Ala-Nissila, and S. C. Ying, *J. Chem. Phys.* **124**, 034714 (2006).
- [24] K. F. Luo, I. Huopaniemi, T. Ala-Nissila, and S. C. Ying, *J. Chem. Phys.* **124**, 114704 (2006).
- [25] I. Huopaniemi, K. F. Luo, T. Ala-Nissila, and S. C. Ying, *J. Chem. Phys.* **125**, 124901 (2006).
- [26] K. F. Luo, T. Ala-Nissila, S. C. Ying, and A. Bhattacharya, *Phys. Rev. Lett.* **99**, 148102 (2007).
- [27] D. S. Wei, W. Yang, X. G. Jin, and Q. Liao, *J. Chem. Phys.* **126**, 204901 (2007).
- [28] Y. C. Chen, C. Wang, and M. B. Luo, *J. Chem. Phys.* **127**, 044904 (2007).
- [29] M. B. Luo, *Polymer* **48**, 7679 (2007).
- [30] M. G. Gauthier and G. W. Slater, *J. Chem. Phys.* **128**, 175103 (2008).
- [31] Y. C. Chen, C. Wang, Y. L. Zhou, and M. B. Luo, *J. Chem. Phys.* **130**, 054902 (2009).
- [32] K. F. Luo and R. Metzler, *Phys. Rev. E* **82**, 021922 (2010).
- [33] M. B. Luo and W. P. Cao, *Phys. Rev. E* **86**, 031914 (2012).
- [34] T. Ambjörnsson, S. P. Apell, Z. Konkoli, E. A. Di Marzio, and J. J. Kasianowicz, *J. Chem. Phys.* **117**, 4063 (2002).
- [35] M. Muthukumar, *J. Chem. Phys.* **132**, 195101 (2010).
- [36] K. E. S. Matlack, W. Mothes, and T. A. Rapoport, *Cell* **92**, 381 (1998).
- [37] W. Neupert and M. Brunner, *Nat. Rev. Mol. Cell. Biol.* **3**, 555 (2002).
- [38] A. B. Fulton, *Cell* **30**, 345 (1982).
- [39] A. Gopinathan and Y. W. Kim, *Phys. Rev. Lett.* **99**, 228106 (2007).
- [40] W. P. Cao, L. Z. Sun, C. Wang, and M. B. Luo, *J. Chem. Phys.* **135**, 174901 (2011).
- [41] W. C. Yu and K. F. Luo, *J. Am. Chem. Soc.* **133**, 13565 (2011).
- [42] W. C. Yu, Y. D. Ma, and K. F. Luo, *J. Chem. Phys.* **137**, 244905 (2012).
- [43] Y. H. Chen and K. F. Luo, *J. Chem. Phys.* **138**, 204903 (2013).

- [44] J. M. Polson and A. C. M. McCaffrey, *J. Chem. Phys.* **138**, 174902 (2013).
- [45] I. Carmesin and K. Kremer, *Macromolecules* **21**, 2819 (1988).
- [46] A. Milchev, *J. Phys.: Condens. Matter* **23**, 103101 (2011).
- [47] W. P. Cao, L. Z. Sun, C. Wang, and M. B. Luo, *Int. J. Mod. Phys. B* **25**, 3345 (2011).
- [48] C. Wang, Y. C. Chen, Y. L. Zhou, and M. B. Luo, *J. Chem. Phys.* **134**, 064905 (2011).
- [49] J. H. Huang, Z. F. Mao, and C. J. Qian, *Polymer* **47**, 2928 (2006).
- [50] M. Bishop and C. J. Saltiel, *J. Chem. Phys.* **88**, 3976 (1988).
- [51] J. H. Huang, M. B. Luo, and S. J. Han, *Chinese J. Polym. Sci.* **21**, 65 (2003).
- [52] M. B. Luo, J. H. Huang, Y. C. Chen, and J. M. Xu, *Eur. Polym. J.* **37**, 1587 (2001).
- [53] R. A. Quinn and J. Goree, *Phys. Rev. Lett.* **88**, 195001 (2002).
- [54] S. Nunomura, D. Samsonov, S. Zhdanov, and G. Morfill, *Phys. Rev. Lett.* **96**, 015003 (2006).
- [55] W. T. Juan and L. I., *Phys. Rev. Lett.* **80**, 3073 (1998).